Peptide−Membrane Interactions Studied by a New Phospholipid/Polydiacetylene Colorimetric Vesicle Assay†

Sofiya Kolusheva, Tamar Shahal, and Raz Jelinek*

Department of Chemistry and Stadler Minerva Center for Mesoscopic, Macromolecular Engineering, Ben Gurion University of the Negev, Beersheva 84105, Israel

Received June 11, 2000; Revised Manuscript Received September 1, 2000

ABSTRACT: Interactions between peptides and lipid membranes play major roles in numerous physiological processes, such as signaling, cytolysis, formation of ion channels, and cellular recognition. We describe a new colorimetric technique for studying peptide−membrane interactions. The new assay is based on supramolecular assemblies composed of phospholipids embedded in a matrix of polydiacetylene (PDA) molecules. The phospholipid/PDA vesicle solutions undergo visible color changes upon binding of membrane peptides. Experiments utilizing various analytical techniques confirm that the blue-to-red color transitions of the phospholipid/PDA vesicles are directly related to adoption of helical conformations by the peptides and their association with the lipids. Spectroscopic data indicate that the colorimetric transitions are correlated with important molecular parameters, such as the degree of penetration of the peptides into lipid bilayers, and the mechanisms of peptide−lipid binding. The results suggest that the new colorimetric assay could be utilized for studying interactions and organization of membrane peptides.

Membrane-associated peptides and proteins participate in diverse biochemical processes, and characterization of the molecular properties of peptide−membrane interactions is highly desirable. Intensive research efforts have been carried out to elucidate the orientations and helical content of transmembrane peptide domains of hormone receptors and ion channels (*1*) and the mechanisms of binding and membrane disruption by short cytolytic peptides (*2*). A variety of structural models describing interactions between short peptides and membranes have emerged in recent years, such as the transmembrane channel aggregates (*3*), the "barrel-stave" model (*4*), and the "carpet" mechanism pertaining to membrane permeation by lytic peptides (*5*).

Development of functional or biochemical assays that provide information upon interactions between membrane peptides and lipid bilayers could contribute to the elucidation of structural and functional properties of the peptides, and their organization in membrane environments. Such assays might also improve screening for new pharmacological substances that function in membrane environments. We describe here a colorimetric assay in which mixed vesicles composed of phospholipids and polymerized polydiacetylene (PDA)[1] lipids are shown to exhibit rapid visible color changes upon interactions with membrane peptides. The blue-to-red colorimetric transitions are directly related to biological association of the peptides with the phospholipid moieties within the vesicles. The results indicate that phospholipid/PDA mixed vesicles could be utilized as a model system for studying peptide−membrane interactions and interfacial membrane processes.

PDA-based vesicles have been previously shown to undergo blue-to-red color transitions induced by a variety of interfacial processes (*6, 7*). Previous studies have revealed that biological processes leading to structural perturbations at the PDA vesicle interface, including ligand−receptor recognition (*8*), pH changes (*7*), and enzymatic catalysis (*9*), are responsible for the blue-to-red transitions occurring in the vesicle assemblies. We have recently demonstrated that PDA vesicles incorporating a high percentage of phospholipid molecules could be used as biosensors for screening of antibacterial peptides (*10*) and for detection of ions in aqueous solutions (*11*).

The peptides investigated in this work include melittin (*12*), melittin analogues (*13*), magainin (*14*), and alamethicin (*15*). These membrane peptides were specifically selected as a "proof of concept" for the colorimetric assay, since they have been extensively characterized in various conditions and membrane environments. The spectroscopic data presented here confirm that the peptides adopt helical conformations in the phospholipid/PDA vesicle environment. Furthermore, we observe a correlation between the degree of blue-to-red colorimetric transitions and the mode of peptide−membrane binding. The results indicate that the phospholipid/PDA assemblies successfully mimic lipid membrane environments, and the assay could discriminate, through evaluation of the colorimetric transitions, between existing models for peptide−membrane interactions.

† Partial financial support from the U.S.-Israel Science Foundation is acknowledged.

* To whom correspondence should be addressed: Department of Chemistry, Ben Gurion University of the Negev, Beersheva 84105, Israel. E-mail: razj@bgumail.bgu.ac.il. Fax: 972-7-6472943. Telephone: 972-7-6461747.

[1] Abbreviations: PDA, polydiacetylene; DMPC, dimyristoylphosphatidylcholine; DMPG, dimyristoylphosphatidylglyerol; DMPE, dimyristoylphosphatidylethanolamine; LPS, lipopolysaccharide; DPPC, dipalmitoylphosphatidylcholine; CD, circular dichroism; NMR, nuclear magnetic resonance; UV, ultraviolet; ESR, electron spin resonance; TFE, trifluoroethanol.

10.1021/bi000570b CCC: $19.00
Published on Web 12/02/2000

MATERIALS AND METHODS

Materials. Phospholipids, including dimyristoylphosphatidylcholine (DMPC), dipalmitoylphosphatidylcholine (DPPC), dimyristoylphosphatidylethanolamine (DMPE), and dimyristoylphosphatidylglycerol (DMPG), were purchased from Avanti Polar Lipids (Alabaster, AL). Sphingomyelin and lipopolysaccharide (LPS) (*Escherichia coli* 055:B5) were purchased from Sigma. The diacetylene monomer tricosadiynoic acid was purchased from GFS Chemicals (Powell, OH). Lipids were washed in chloroform and water and filtered through 0.8 μm filters. Preparation of vesicles containing phospholipids and PDA (2:3 mole ratio) has been described previously (*9*, *11*). Briefly, the lipid constituents are dried together in a vacuum, followed by addition of deionized water and probe sonication at ~70 °C. The vesicle solution is then cooled, kept at 4 °C overnight, and polymerized using irradiation at 220 nm. The resulting solution exhibits an intense blue appearance.

Melittin (GIGAVLKVLTTGLPALISWIKRKRQQ) and magainin II (GIGKFLHSAKKFGKAFVGEIMNS) have been synthesized using solid-phase peptide synthesis and purified to >95% using reverse-phase HPLC. Alamethicin has been purchased from Sigma. The more abundant alamethicin homologue containing glutamic acid at position 18 (AibPAibAAibAQAibVAibGLAibPVAibAibEQF-OH, where Aib denotes α-aminoisobutyric acid) has been used following separation by HPLC. Melittin analogues were synthesized by Alpha Diagnostics Inc. (San Antonio, TX) using standard Fmoc chemistry. The identity of peptides was confirmed by mass spectrometry and amino acid analysis. Peptides were purified to >95% using reverse-phase HPLC. The melittin diastereomer (D-melittin), containing D-amino acids (Val-5, Val-8, Ile-17, and Lys-21), has been kindly provided by Y. Shai (Weizmann Institute of Science, Rehovot, Israel). The M2 domain of the δ subunit of the acetylcholine receptor (AchR) (sequence EKMSTAISVLLAQAVFLLLTSQR) has been generously provided by S. Opella (University of Pennsylvania, Philadelphia, PA).

UV−Vis Measurements. Samples were prepared by adding peptides to 0.4 mL vesicle solutions at 1 mM total lipid and 2 mM Tris. The pH in the solutions was 8.5 in all experiments. Melittin, melittin analogues, and magainin were dissolved in water, while alamethicin and the M2 peptide were dissolved in TFE (control experiments verified that the background red color induced by TFE only is negligible). Following addition of the peptides, the solutions were diluted to 1 mL and the spectra were acquired. All measurements have been carried out at 27 °C on a Hewlett-Packard 8452A diode-array spectrophotometer, using a 1 cm optical path length cell.

A quantitative value for the extent of blue-to-red color transition is given by the colorimetric response (%CR), which is defined (*9*)

$$\%CR = [(PB_0 - PB_I)/PB_0] \times 100$$

where $PB = A_{blue}/(A_{blue} + A_{red})$, A is the absorbance at either the "blue" component in the UV−vis spectrum (≈640 nm) or the "red" component (≈500 nm), PB_0 is the red/blue ratio of the control sample (before induction of color change), and PB_I is the value obtained for the vesicle solution after addition of peptides.

Circular Dichroism Experiments. CD spectra were acquired on an Aviv 62A-DS circular dichroism spectrometer (Aviv Inc.). Four scans were recorded between 190 and 250 nm with 1 nm acquisition steps. A 0.2 mm optical path length was used. All vesicle solutions had a total lipid concentration of 1 mM (40% mol % DMPC) in 2 mM Tris at pH 8.5. Peptide concentrations were 0.1 mM. Fractional helicities (f_h) were calculated as (*16*)

$$f_h = (\theta_{222} - \theta^0_{222})/(\theta^{100}_{222} - \theta^0_{222})$$

where θ_{222} is the experimentally observed elipticity at 222 nm, θ^0_{222} corresponds to 0% helical content (determined for 0.1 mM melittin in deionized water to be −7000 deg cm^2 dmol^{-1}), and θ^{100}_{222} corresponds to 100% helical content (−41000 deg cm^2 dmol^{-1} for melittin in 80% TFE).

Fluorescence Measurements. Changes in tryptophan intrinsic emission were measured for 10 μM peptide solutions titrated with DMPC/PDA vesicles. Fluorescence emission spectra were acquired at 27 °C on a SLM Aminco Bowman spectrofluorimeter, using excitation at 280 nm and emission at 345 nm. Excitation and emission slits were both 8 nm. Total sample volumes were 1 mL, and the solutions were placed in a quartz cell having a 0.5 cm optical path length. Light scattering from the vesicles was confirmed to account for less than 5% of the emission intensity.

NMR. ^{13}C NMR spectra were acquired using 1 mM (total lipid concentration) DMPC/PDA vesicle solutions, prepared using DMPC isotope-labeled with ^{13}C at both carbonyl positions (Avanti Polar Lipids). Peptide concentrations were 0.2 mM. Spectra were acquired at a magnetic field of 11.7 T on a Bruker DMX500 NMR spectrometer. Five thousand scans were accumulated for each spectrum using a Bloch-decay pulse sequence with recycle delay of 1 s. A 10 Hz Lorentzian window function has been applied to all spectra. TMS was the external reference.

Electron Spin Resonance. Samples for the ESR experiments were prepared using spin probes 5-doxylstearic acid (5-DS) and 12-doxylstearic acid (12-DS) purchased from Sigma. The spin probe fatty acid was added to the vesicle samples after the polymerization step, in a molar ratio of 1:100 (spin probe:phospholipid). Samples were placed in a 20 mm length, 1 mm inside diameter quartz capillary and recorded using a Bruker EMX-220 digital X-band spectrometer at 25 °C. The amplitudes of 12.5 and 100 kHz, the modulation, and the microwave power level were chosen at subcritical values (0.5 G and 20 mW, respectively) to reach the best signal:noise ratio. Processing of the ESR spectra (digital filtering, double integration, etc.) was carried out using Bruker WIN-EPR software.

RESULTS AND DISCUSSION

DMPC/PDA mixed vesicles have been prepared using approximately 40% (mole ratio) of phospholipids, such as DMPC, and 60% polydiacetylene (PDA) lipids. Following sonication and polymerization, the lipids form organized assemblies, which exhibit an intense blue color due to the conjugated backbone of the PDA polymer (*17*). Figure 1 presents a schematic drawing of the phospholipid/PDA assembly. The phospholipid molecules are distributed within the conjugated PDA matrix, and most likely exist in a

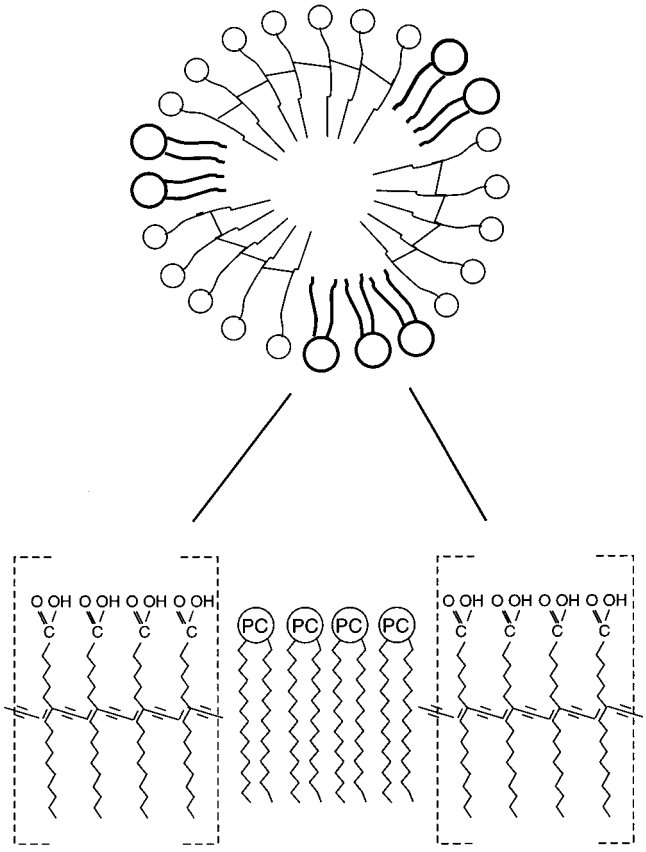

FIGURE 1: Schematic representation of the phospholipid/PDA vesicles, indicating a part of the assembly of phospholipids and polydiacetylene. PC denotes the phosphatidylcholine headgroup.

domain-like configuration. This arrangement is inferred both from statistical analysis of phospholipid distribution within the vesicles and from experimental data obtained for PDA/phospholipid thin films (F. Gaboriaud and R. Jelinek, manuscript in preparation). Previous characterization of the phospholipid/PDA system also points to a similar picture (*10*). The conjugated PDA backbone absorbs light in the visible region, resulting in a blue appearance of the vesicle solution. Biochemical events leading to physical or chemical disruption of the phospholipid assembly give rise to the blue-to-red colorimetric transitions, induced, most likely, through structural perturbations of the adjacent PDA network (*6*, *11*).

Color changes induced upon mixing membrane peptides with the phospholipid/PDA vesicle solutions are shown in Figure 2. Figure 2A depicts a photograph of part of a 96-well plate containing DMPC/PDA vesicles, into which several membrane peptides have been separately added. The extent of colorimetric transitions is generally affected by the quantity of peptide added to the solution (*10*). The peptide concentrations used in Figure 2A were adjusted to obtain an equal number of membrane-bound peptides in each well, taking into account the respective partition coefficients of the peptides (*18*). While the peptide concentrations used in the experiments whose results are depicted in Figure 2 allow visible detection of the color changes by the naked eye, it should be noted that, in general, colorimetric transitions can be detected in much lower concentrations (micromolar) using UV−vis spectroscopy (*10*). The color changes observed in Figure 2A clearly indicate that the peptides interact with the vesicles. The different degree of colorimetric transitions observed following addition of each peptide is attributed to

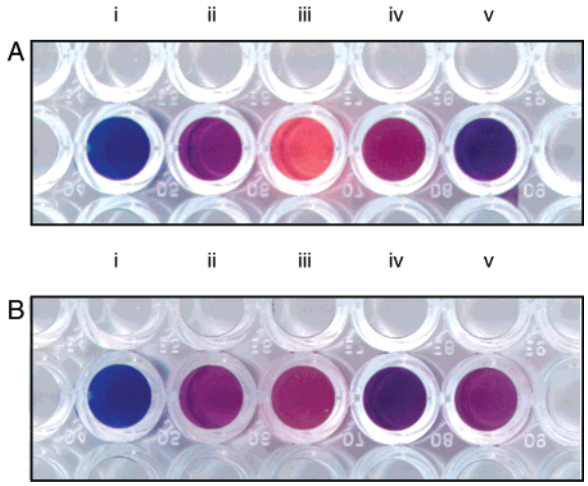

FIGURE 2: (A) Photograph of DMPC/PDA solutions, at 27 °C after addition of peptides: (i) control (no peptide), (ii) melittin (0.1 mM), (iii) magainin (1 mM), (iv) alamethicin (0.1 mM), and (v) M2 domain of the AchR protein (0.15 mM). Each cell contained 100 μL of a 1 mM (total lipid concentration) DMPC/PDA (4:6 mole ratio) and 2 mM Tris solution at pH 8.5. (B) Photograph of phospholipid/PDA solutions after addition of melittin. The total lipid concentration in all wells was 1 mM, and the peptide concentration was approximately 0.1 mM: (i) control (DMPC/PDA vesicles, no melittin added), (ii) DMPC/PDA (2:3 mole ratio), (iii) sphingomyelin/DMPC/PDA (1:1:3 mole ratio), (iv) DMPE/DMPG/PDA (3:1:6 mole ratio), and (v) LPS/DMPC/PDA (1:4:6 mole ratio).

the distinct mechanisms of peptide−membrane interactions (see below). Soluble peptides, which are not expected to associate with lipid membranes, do not induce blue-to-red color changes within the phospholipid/PDA vesicles (*10*).

Blue-to-red colorimetric transitions are induced by interactions of membrane peptides with PDA vesicles containing various natural lipid components. Figure 2B, for example, shows that melittin generates color changes in vesicles incorporating zwitterionic and negatively charged phospholipids, sphingolipids, and glycolipids. The lipid ratios presented in Figure 2B are typical for various mammalian and bacterial membranes (*1*, *19*). The different color changes observed in Figure 2B most likely depend on the size and charge of the lipid headgroups, which affect the binding and the degree of penetration of the peptide into the lipid assembly (*20*). The general applicability of the assay for detection of peptide interactions with vesicles containing diverse lipid building blocks is important, since the lipid composition of membranes is one of the most important parameters that determine membrane properties and peptide−membrane interactions (*19*). Quantification of the colorimetric transitions induced by membrane peptides in phospholipid/PDA vesicles is also feasible, based upon the UV−vis spectra of individual solutions (*10*). A previous study has indicated that the phospholipid/PDA system can detect peptide concentrations in the micromolar range (*10*).

Several experiments have been carried out to investigate the binding of the peptides and to evaluate the biological significance of the colorimetric transitions. UV−vis absorbance spectra shown in Figure 3 confirm that the observed color changes are directly related to specific association of the peptides with the embedded phospholipids within the PDA matrix, rather than the PDA molecules themselves. Figure 3A shows that the blue-to-red color change, induced by melittin, depends on the presence of DMPC within the

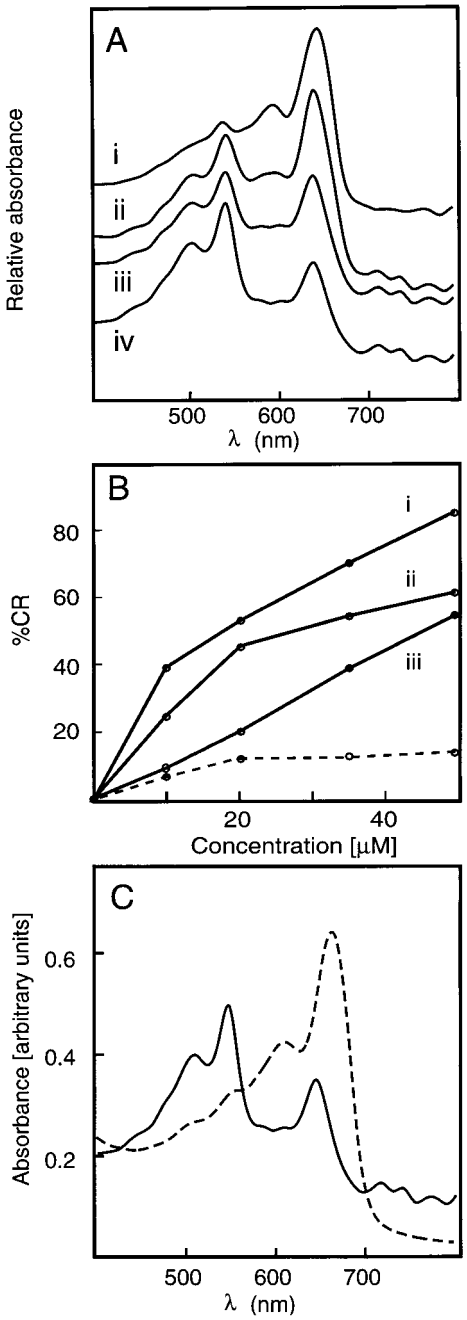

FIGURE 3: UV−vis data of vesicle solutions mixed with peptides. (A) UV−vis spectra of melittin: (i) control solution (blue PDA vesicles) with no peptide added, (ii) melittin added to pure PDA vesicles (100% polydiacetylene, no DMPC), (iii) melittin added to DMPC/PDA vesicles in a 2:8 mole ratio, and (iv) melittin added to DMPC/PDA vesicles in a 4:6 mole ratio. The total lipid concentration was 1 mM, and the melittin concentration was 0.03 mM in all samples. (B) Colorimetric response (%CR). Graph depicting the changes in colorimetric response (see the definition in Materials and Methods) upon titration of vesicles with membrane peptides: (i) magainin, (ii) melittin, and (iii) alamethicin. The vesicles that were examined were DMPC/PDA vesicles (2:3 mole ratio). The dashed line shows the results with melittin added to pure PDA (100%) vesicles. The total lipid concentrations in all vesicle samples were 1 mM. (C) UV−vis spectra: (—) melittin added to DMPC/PDA vesicles (4:6 mole ratio) and (- - -) melittin added to DPPC/PDA vesicles (4:6 mole ratio). The melittin concentration was 0.03 mM, and the total lipid concentration was 1 mM.

vesicles. This is apparent in the UV−vis spectra, as the ratio between the absorbance at ∼500 nm (the red band in the UV−vis spectrum) and 640 nm (the blue band) increases with the percentage of phospholipids in the vesicles (note that blue and red refer to the visual appearance of the material, not its actual absorbance).

This observation is also demonstrated in Figure 3B, which depicts titration curves of the membrane peptides alamethicin, melittin, and magainin added to mixed DMPC/PDA vesicles. The quantitative colorimetric response (%CR) data shown in Figure 3B indicate that the color changes are directly related to the concentrations of the added peptide. However, the blue-to-red color changes are much more pronounced (higher %CR) when the peptides are mixed with vesicles that contain phospholipids. This result again indicates that melittin preferably binds to the phospholipid moieties, rather than the polymer matrix. The small background color change detected when melittin, for example, is added to pure PDA vesicles (broken line in Figure 3B) is attributed to electrostatic interactions of the peptide with charged headgroups of the polymerized lipid (*10*). It should be emphasized that the observation of significantly stronger color transitions when DMPC/PDA vesicles are employed, compared to pure PDA, supports the proposal that the colorimetric effects are indeed biologically relevant, rather than due to electrostatic binding of the peptides to the PDA interface.

Further evidence for the above interpretation is provided by analysis of the colorimetric transitions induced by melittin in PDA vesicles containing different phospholipids. UV−vis data shown in Figure 3C indicate that, at 27 °C, vesicles containing dipalmitoylphosphatydilcholine (DPPC) rather than DMPC do not undergo blue-to-red color transition upon addition of melittin. This result is consistent with the expectation that melittin would not associate with DPPC at 27 °C, since this phospholipid exists in the gel phase at that temperature (*12*). The observation of a much smaller color change after addition of melittin to DPPC/PDA, compared to DMPC/PDA, vesicles is significant, because DPPC differs from DMPC only in the length of the fatty chains, and the two molecules have identical structures otherwise. Accordingly, the colorimetric data in Figure 3C clearly demonstrate that the color changes are directly related to the interaction of the peptide with phospholipid molecules within the vesicles.

Panels A−C of Figure 4 depict circular dichroism (CD) spectra recorded for melittin, magainin, and alamethicin, respectively, in water and in aqueous mixtures containing DMPC/PDA vesicles. The three examined peptides do not adopt detectable secondary structures in solutions having low salt concentrations and at slightly basic pH (*12*, *21*). Panels A−C of Figure 4 reveal, however, that melittin, magainin, and alamethicin acquire significant helical structures in aqueous solutions containing DMPC/PDA vesicles, which is apparent from the easily identified minima at ∼208 and 220 nm, respectively, in the CD spectra. These results are consistent with previous studies indicating that the three peptides studied here, in particular, and membrane peptides, in general, are mostly unstructured in aqueous solutions, while they adopt helical conformations in the presence of organized lipid assemblies (*21*, *22*).

Further evidence for a direct relationship between the acquisition of helical structure and the interaction between the peptides and the DMPC/PDA assembly is provided in Figure 4D. Figure 4D presents the extent of helical content

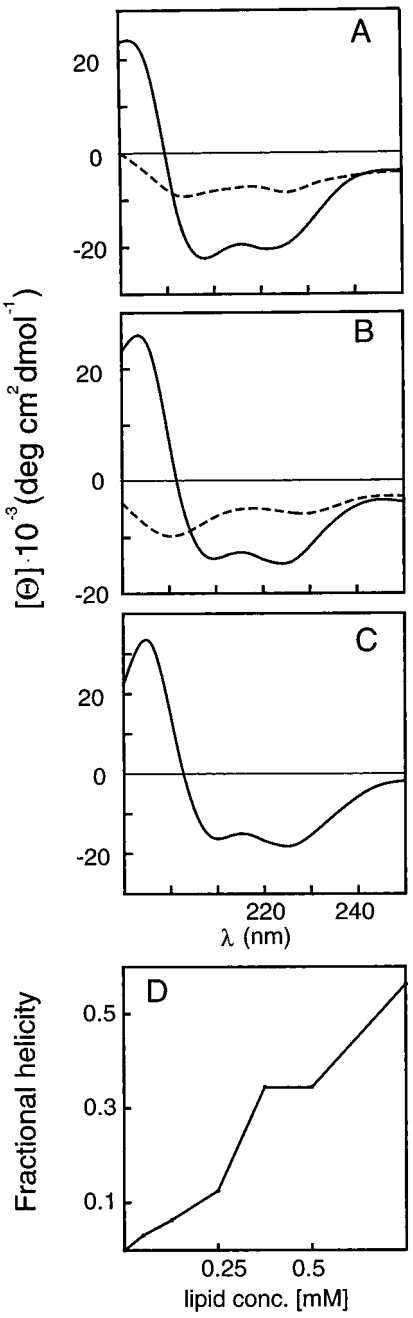

FIGURE 4: CD spectra of peptide solutions. (A) Melittin: (- - -) melittin in aqueous solution (2 mM Tris at pH 8.5) and (—) melittin added to a DMPC/PDA solution. (B) Magainin: (- - -) magainin II in aqueous solution (2 mM Tris at pH 8.5) and (—) magainin II added to a DMPC/PDA solution. (C) Alamethicin (dissolved in trifluoroethanol) added to a DMPC/PDA solution (no CD spectrum available in aqueous solution due to aggregation of alamethicin). All vesicle solutions had total lipid concentrations of 1 mM (40% mol % DMPC) and in 2 mM Tris at pH 8.5. Peptide concentrations in the CD experiments were 0.1 mM. (D) Graph depicting the fractional helicity of melittin, calculated from the CD data, as a function of lipid concentration.

of melittin as a function of vesicle concentration and clearly demonstrates that the addition of DMPC/PDA vesicles to the peptide solution results in higher helical contents for the peptide. The highest helicity value depicted in the graph (~60%) corresponds to a %CR of ~55% (see Figure 3B), indicating that the color transition is indeed due to the helical association of the peptide with the lipid assembly. Similar results were obtained for the other membrane peptides that

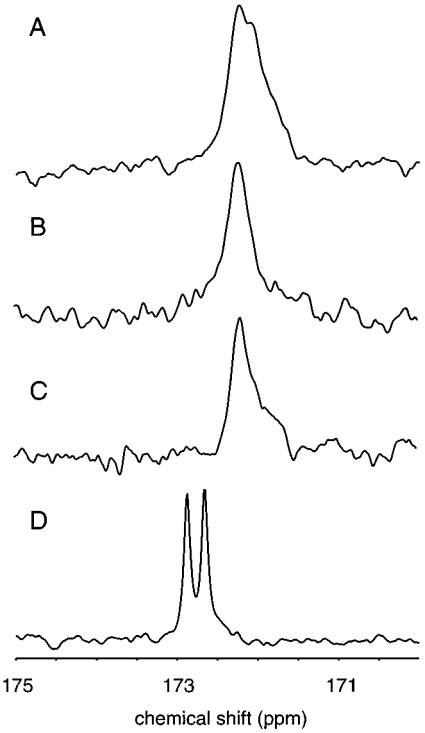

FIGURE 5: ^{13}C NMR spectra of the carbonyl region of DMPC/PDA vesicle solutions, prepared using DMPC isotope-labeled with ^{13}C at both carbonyl positions: (A) DMPC/PDA vesicles with no peptide added, (B) melittin added, (C) magainin II added, and (D) alamethicin added. The total lipid concentration was 1 mM in all samples, and the peptide concentration was 0.1 mM.

were investigated. The CD data shown in Figure 4 are significant, since the induction of helical structures in the present of the mixed lipid/polymer vesicles confirms that the phospholipid domains incorporated within the PDA matrix essentially mimic the lipid−membrane interface.

^{13}C NMR data, shown in Figure 5, are consistent with the UV−vis and CD spectroscopic results, and provide further evidence that the blue-to-red color changes are due to specific interactions between the peptides and phospholipids. Figure 5 depicts ^{13}C NMR spectra of PDA vesicles containing DMPC molecules isotope-labeled with ^{13}C at both carbonyl positions. The ^{13}C spectrum shown in Figure 5A corresponds to the two overlapping carbonyl signals from the DMPC molecules embedded within the PDA matrix. All three peptides affect the carbonyl ^{13}C resonances. Addition of melittin and magainin results in narrowing of the spectral line, either through interaction of the peptides with one of the carbon sites or due to the increased mobility of the carbon nuclei. Motional narrowing of ^{31}P resonances in melittin/phospholipid vesicles has been previously observed (*23*). Addition of alamethicin, in particular, gives rise to two sharp downfield-shifted ^{13}C signals (Figure 5D), which most likely correspond to the two isotope-labeled carbonyl positions within DMPC. The narrow resonances observed in the ^{13}C spectrum after addition of alamethicin imply that highly mobile DMPC molecular species are formed following interaction of the peptide with the vesicles, possibly through micellization (*24*). Dynamic light scattering measurements of the DMPC/PDA solutions (data not shown) indicate that the vesicles become significantly smaller in the presence of alamethicin. The changes observed in the ^{13}C carbonyl spectra suggest that interactions of the membrane peptides

examined in this work result in modifications of the local environments and dynamics of the phospholipid molecules within the PDA matrix.

Further insight into the relationships between the observed colorimetric transitions in the vesicle solutions, and the mechanisms of peptide−membrane interactions, is obtained from examination of peptide analogues, in which the native amino acid sequences have been modified. In the work presented here, we examine melittin analogues in which amino acids located in functionally and structurally important positions in the sequence have been substituted or omitted (*13*, *25*). An additional melittin analogue was investigated in which certain L-amino acids have been replaced with the corresponding D-amino acids [denoted D-melittin (*26*, *27*)]. These analogues have previously provided a wealth of structural and functional information about the amino acid sequence of melittin and its membrane interactions.

Figure 6A shows a photograph of the color changes induced in DMPC/PDA vesicle solutions by melittin and melittin analogues, which were added in identical concentrations. All melittin analogues that are shown induce more reddish colors, compared to native melittin [Figure 6A (wells ii−v)]. A melittin diastereomer, in which residues Val-5 and -8, Ile-17, and Lys-21 have been replaced with the D-amino acids, was added to well iii in Figure 6A. Well iv in Figure 6A contains an analogue in which Trp-19 has been omitted (denoted ΔW19-melittin), while a melittin analogue where Leu-9 has been substituted with lysine (subL9K-melittin) has been added to the vesicles in well v in Figure 6A. Further evidence for the more pronounced colorimetric transitions induced by D-melittin, compared to those with L-melittin, is provided in Figure 6B, which features the titration curves of L-melittin and D-melittin. The colorimetric data shown in Figure 6B indicate that, most likely, there exists a difference between the mechanisms of colorimetric transitions induced by L-melittin and D-melittin.

The structural modifications of the melittin sequence in the analogues examined in Figure 6 prevent adoption of the complete helical conformation by the peptides (*26*−*28*). This is also confirmed in the CD spectra shown in Figure 6C, which indicate that the melittin analogues exist in a mostly extended conformation in the presence of DMPC/PDA vesicles, as opposed to the helical conformation of native melittin. Thus, these melittin analogues cannot penetrate into the hydrophobic alkyl core of the phospholipid assemblies, but rather bind at the lipid−water interface, mostly through electrostatic interactions (*28*, *29*). This interpretation could explain the more pronounced blue-to-red colorimetric transitions induced by the analogues, as compared to the native melittin sequence (Figure 6). In general, the colorimetric transitions observed in the phospholipid/PDA vesicle assemblies correspond to rearrangement of the pendant PDA side chains, induced by interfacial perturbations at the phospholipid domains (*6*, *10*). Accordingly, it is expected that association of peptides, such as D-melittin (*26*), at the surface of the lipid assemblies would induce greater interfacial perturbations, and thus a more extreme color change, compared to transmembrane insertion of a helical peptide, such as melittin, into the lipid assemblies. This model also successfully accounts for the color transitions induced by the peptides depicted in Figure 2A. The M2 domain of the AchR, for example, which inserts vertically into lipid bilayers

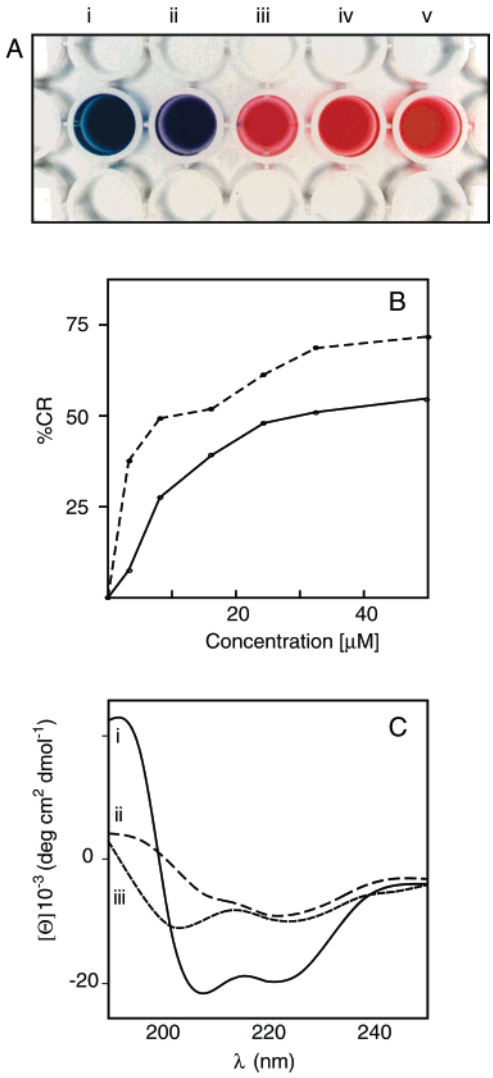

FIGURE 6: (A) Photograph of DMPC/PDA solutions, at 27 °C, after addition of melittin and melittin analogues: (i) control solution (no peptide added), (ii) L-melittin, (iii) D-melittin, (iv) ΔW19-melittin, and (v) subL9K-melittin. (B) Titration curves depicting the change of the colorimetric response (%CR) as a function of peptide concentration: (—) L-melittin and (- - -) D-melittin. (C) CD spectra of (i) L-melittin, (ii) ΔW19-melittin, and (iii) SubL9K-melittin. The solutions in the cells photographed and in the CD experiments had a total lipid concentration of 1 mM in 2 mM Tris buffer at pH 8.5. Peptide concentrations were ∼0.1 mM.

(*30*), gives rise to a purple color in the vesicle solution (well V in Figure 2A). However, a significantly more pronounced red-orange color is induced by magainin (well iii in Figure 2A), since magainin is an amphipathic peptide spanning the water−lipid interface in membrane environments (*18*, *31*).

The apparent relationship between the colorimetric response of the phospholipid/PDA assay and the mechanism of peptide−membrane association is an important contribution for studying peptide−membrane interactions and organization. Figures 7−9 present independent spectroscopic measurements that further confirm the correlation between the colorimetric responses with fundamental biophysical parameters pertaining to peptide−membrane interactions, such as the mode of peptide binding and the extent of insertion of the peptides into lipid bilayers.

Figure 7 illustrates tryptophan fluorescence spectra of peptides in solutions containing DMPC/PDA vesicles. The

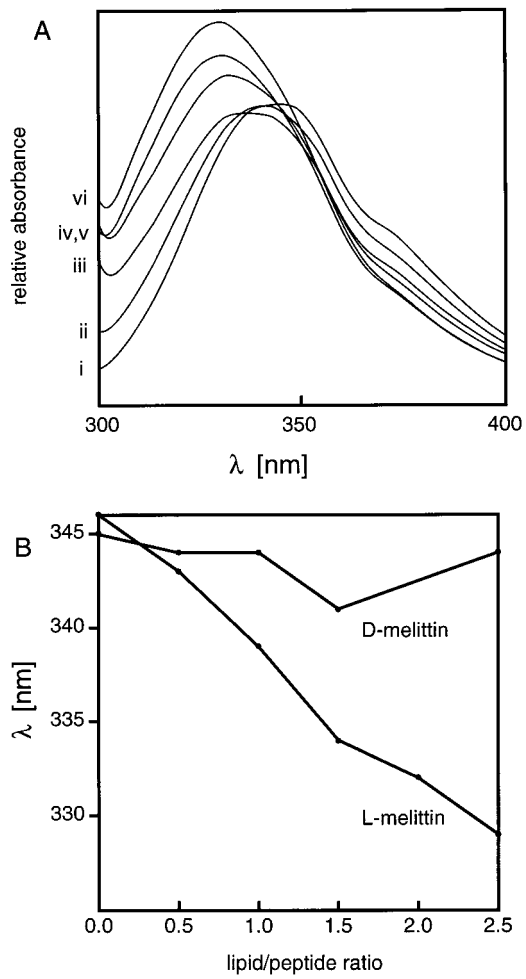

FIGURE 7: Tryptophan fluorescence data of melittin and melittin analogues added to 1 mM DMPC/PDA vesicles. (A) Emission spectra of melittin at different lipid:peptide ratios: (i) 0, (ii) 0.5, (iii) 1, (iv) 1.5, (v) 2, and (vi) 2.5. (B) Graph depicting the change in the shift of the emission peak at different lipid:peptide ratios for L-melittin and D-melittin.

data shown in Figure 7 clearly indicate that there is a significant difference between the degree of penetration of native melittin (L-melittin) into the hydrophobic core of the lipids and the D-melittin diastereomer which cannot adopt a complete helical structure (*26*, *27*). Melittin has a single tryptophan residue at position 19 (Trp-19), commonly used as a fluorescent probe for studying melittin−membrane interactions (*32*, *33*). Figure 7A, for example, demonstrates that, in the case of native melittin, higher lipid-to-peptide ratios give rise to both an increase in the intensity of the Trp fluorescence emission signal and a shift of the peak to lower wavelengths. These changes are indicative of membrane insertion of melittin, and correspondingly a more hydrophobic environment, on average, for Trp-19, which diminishes the level of fluorescence quenching occurring in aqueous surroundings (*33*).

Figure 7B graphically displays the changes in the spectral position of the tryptophan fluorescence signal as a function of the lipid:peptide ratio, in L-melittin and D-melittin. Figure 7B demonstrates that while the Trp-19 signal in L-melittin is shifted to lower wavelengths, the fluorescence peak in D-melittin does not exhibit the same shift. This result indicates that the single tryptophan residue in D-melittin experiences a significantly less hydrophobic environment

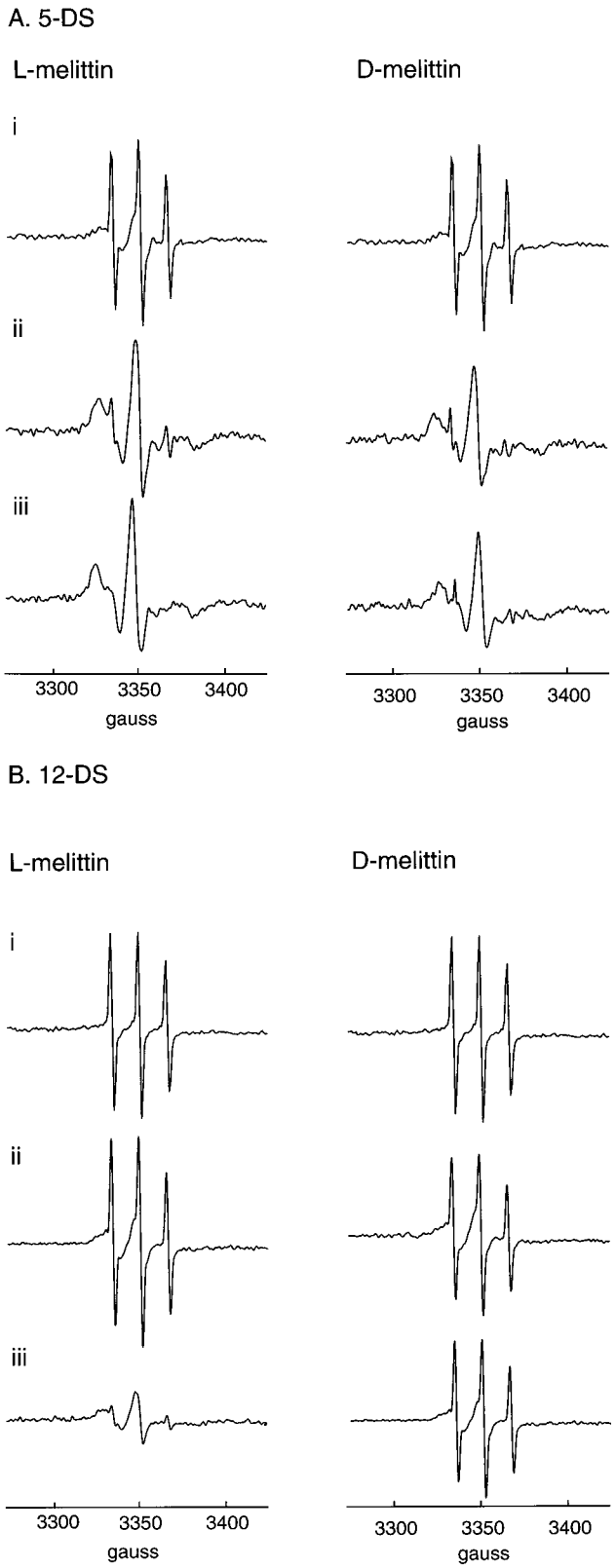

FIGURE 8: ESR spectra obtained for the nitroxide-labeled fatty acids, in which the spin probe has been attached at the carbon 5 and 12 positions at the acyl chain and incorporated in DMPC/PDA vesicles (total lipid concentration of 1 mM): (A) 5-DS and (B) 12-DS. The peptide:lipid ratios were (i) 0, (ii) 0.05, (iii) 0.1.

than the Trp-19 in L-melittin. These data are again consistent with the established model indicating the inability of D-melittin to fully insert into lipid bilayers, due to its incomplete folding into a helical structure (*27*, *29*). Previous studies have

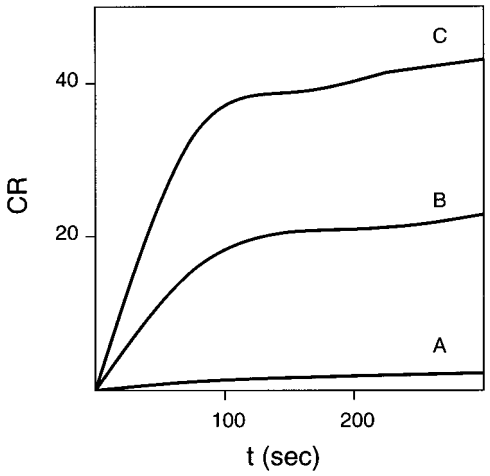

FIGURE 9: Curves depicting the time evolution of the colorimetric response (see the definition in Materials and Methods) of DMPC/PDA vesicles at 27 °C: (A) control (no peptide), (B) melittin, and (C) magainin. The solutions had a total lipid concentration of 1 mM in 2 mM Tris buffer at pH 8.5. Peptide concentrations were ~10 μM.

determined that D-melittin attains helical structure in less than 20% of the total sequence (*27*); consequently, the energy cost for its partitioning into the hydrophobic core of the lipids is very high, which effectively prevents its penetration beyond the lipid−water interface (*34*). The attachment and aggregation of D-melittin onto the lipid−water surface results in a greater interfacial perturbation, both to the lipids and to the pendant side chains of PDA, giving rise to more extreme colorimetric transitions.

Electron spin resonance (ESR) data, shown in Figure 8, provide additional insight into the association of the peptides with the vesicles, and the effect of peptide binding upon the lipid environments. ESR spectra were acquired using phospholipid/PDA vesicles incorporating stearic acid to which the spin probe doxyl residue has been covalently attached in carbon positions 5 and 12 in the acyl chain. Spin-labeled lipid probes have been extensively used as a tool for probing the organization and local motion within lipid membranes (*35*−*37*). The molar ratio of 100:1 (phospholipid:probe) used in the experiments most likely does not alter the properties and organization of the phospholipid/PDA vesicles. The colorimetric properties of the vesicles were not affected by addition of the spin-labeled probe.

The ESR data shown in Figure 8A indicate that, in vesicles containing 5-doxylstearic acid (5-DS), a broad spectral component which exhibits a greater outer hyperfine splitting is observed following addition of L-melittin or D-melittin to the vesicles. The wider splitting is detected in vesicle solutions containing peptide concentrations of ~50 μM (well ii in Figure 8). The %CR values calculated for such concentrations were 53 and 73% for L-melittin and D-melittin, respectively. The broad component corresponds to a population of spin-labeled probes exhibiting restricted chain mobility, resulting in a decrease in the degree of anisotropic motional averaging (*36*). Previous ESR studies have detected similarly significant restriction of local lipid motion following melittin binding in various model membrane systems (*36*).

Figure 8B reveals that, in contrast to the ESR data acquired for the 5-DS probe which were discussed above, when the doxyl probe is located in carbon position 12 within the acyl chain, the ESR spectra are affected differently by L-melittin and D-melittin. L-Melittin, on one hand, gives rise to a population of motionally restricted spin-labeled probe, apparent from the emerging broad component with a higher hyperfine splitting (well iii in Figure 8B). D-Melittin, on the other hand, does not affect the chain mobility of the spin-labeled lipid probe. The absence of spectral changes even after adding D-melittin up to a concentration of 100 μM (well iii in Figure 8B) is striking, since at that concentration the %CR of the solution approaches 90%. This result again indicates that D-melittin does not penetrate into the hydrophobic core of the lipid assembly, and the colorimetric transition induced by the peptide is due to the interfacial interactions of the peptide. The divergent ESR results shown in Figure 8B for L-melittin and D-melittin provide strong evidence that native L-melittin inserts into the hydrophobic core of the phospholipids, thus restricting the mobility of the spin-labeled probe in a chain position farther away from the lipid−water interface. D-Melittin, however, is bound at the lipid interface, and therefore hardly affects the dynamic properties of the spin-labeled probe at carbon position 12. These conclusions are consistent with the tryptophan fluorescent data discussed above (Figure 7). A similar decrease in the level of lipid motion upon association of ion−ionophore complexes with DMPC/PDA vesicles was previously observed (*11*).

The color changes induced by membrane-associated peptides in phsopholipid/PDA vesicles open additional avenues for studying peptide−membrane interactions. Figure 9, for example, illustrates UV−vis kinetic data, quantitatively depicting the blue-to-red color changes of the vesicle solutions following addition of melittin and magainin. The curves shown in Figure 9 trace the time evolution of the relative intensities of the blue component in the UV−vis absorance spectrum at 640 nm and the red component of the spectrum at ~500 nm. Examination of the dynamical data in Figure 9 reveals that the colorimetric change induced by melittin occurs at a significantly slower rate than the color transition caused by magainin (Figure 9B,C). This result could point to the intrinsic differences between the rate of melittin helix formation and penetration in a transmembrane orientation into the lipid assembly and the level of binding of magainin at the lipid−water interface (*1*, *18*). Further analysis of the data and their relationships with kinetic models is currently under way.

CONCLUSIONS

This work describes a new colorimetric assay that allows screening and characterization of peptide−membrane interactions and organization. The assay is based upon generation of blue-to-red colorimetric transitions in vesicles composed of phospholipids and polydiacetylene lipids. An important goal of the paper has been to evaluate the validity and biochemical relevance of the technique. Accordingly, several analytical and spectroscopic methods have been employed in characterizing the binding and organization of both the peptides, as well as the vesicle assemblies. The experimental data presented indeed verify that the colorimetric responses of the system are biologically important; the peptides that have been studied specifically interact with the phospholipid domains in the vesicles, and they adopt helical conformations in the phospholipid/PDA environments. Significantly, the

data demonstrate the existence of direct relationships between the color changes and the mechanisms of peptide−membrane association. In particular, a relationship has been observed between the colorimetric transitions and the extent of membrane penetration by the peptide; more extreme blue-to-red transitions are induced by peptides which strongly bind at the lipid−water interface, compared with peptides penetrating into the hydrophobic cores of lipid membranes. It should be emphasized, however, that the distinction between the peptide interaction mechanisms, using the colorimetric assay, is feasible only when the relative water−lipid partition coefficients of the peptides being examined have been predetermined. Experimental procedures for rapid evaluation of the partition coefficients in the DMPC/PDA vesicular system are currently being developed.

The induced color changes occur rapidly after addition of the membrane peptides to the solutions containing the phospholipid/PDA vesicles. The assay is robust and can be easily expanded to include a variety of membrane models; vesicles can incorporate phospholipids with various headgroups, glycolipids, sterols, and other membrane constituents. This colorimetric assay might easily be applied for rapid screening of the activities of membrane peptides, and could provide a wealth of structural and functional information about peptide−membrane interactions and mechanisms of membrane permeability. Application of the phospholipid/PDA system for studying the structures and function of larger membrane proteins should be feasible as well.

ACKNOWLEDGMENT

We gratefully acknowledge Professor E. Haas and Dr. Y. Gussakowski (Bar Ilan University, Ramat Gan, Israel) for help with the CD measurements, E. Lozinsky and Dr. A. I. Shames (Ben Gurion University of the Negev) for assistance with the ESR experiments, and Professor Y. Shai (Weizmann Institute for Science) for helpful discussions and providing the D-melittin.

REFERENCES

1. White, S. H. (1994) *Membrane Protein Structure, Experimental Approach*, Oxford University Press, New York.
2. Shai, Y. (1995) *Trends Biochem. Sci. 20*, 460−464.
3. White, J. M. (1992) *Science 258*, 917−924.
4. Ojcius, D. M., and Young, J. D. E. (1991) *Trends Biochem. Sci. 16*, 225−229.
5. Gazit, E., Boman, A., Boman, H. G., and Shai, Y. (1995) *Biochemistry 34*, 11479−11488.
6. Okada, S., Peng, S., Spevak, W., and Charych, D. H. (1998) *Acc. Chem. Res. 31*, 229−239.
7. Cheng, Q., and Stevens, R. C. (1998) *Langmuir 14*, 1974−1976.
8. Charych, D. H., Nagy, J. O., Spevak, W., and Bednarski, M. D. (1993) *Science 261*, 585−588.
9. Jelinek, R., Okada, S., Norvez, S., and Charych, D. (1998) *Chem. Biol. 5*, 619−629.
10. Kolusheva, S., Boyer, L., and Jelinek, R. (2000) *Nat. Biotechnol. 18*, 225−227.
11. Kolusheva, S., Shahal, T., and Jelinek, R. (2000) *J. Am. Chem. Soc. 122*, 776−780.
12. Dempsey, C. E. (1990) *Biochim. Biophys. Acta 1031*, 143−165.
13. Perez-Paya, E., Houghten, R. A., and Blondelle, S. E. (1995) *J. Biol. Chem. 270*, 1048−1056.
14. Zasloff, M. (1987) *Proc. Natl. Acad. Sci. U.S.A. 84*, 5449−5453.
15. LaTorre, R., and Alvarez, O. (1981) *Physiol. Rev. 61*, 77−150.
16. Wu, C. S. C., Ikeda, K., and Yang, J. T. (1981) *Biochemistry 20*, 566−570.
17. Bloor, D., and Chance, R. R., Eds. (1985) *Polydiacetylenes Synthesis, Structure, and Electronic Properties*, Vol. 102, Martinus Nijhoff Publishers, Dordrecht, The Netherlands.
18. Matsuzaki, M., Murase, O., Tokuda, H., Funakoshi, S., Fujii, N., and Niyajima, K. (1994) *Biochemistry 33*, 3342−3349.
19. Merz, K. M., and Roux, B., Eds. (1996) *Biological Membranes, A Molecular Perspective from Computation and Experiment*, Birkhauser, Boston.
20. Heller, W. T., He, K., Ludtke, S. J., Harroun, T. A., and Huang, H. W. (1997) *Biophys. J. 73*, 239−244.
21. Vogel, H. (1987) *Biochemistry 26*, 4562−4572.
22. Thiaudiere, E., Siffert, O., Talbot, J., Bolard, J., Alouf, J. E., and Dufourcq, J. (1991) *Eur. J. Biochem. 195*, 203−213.
23. Beschiaschvili, G., and Baeuerle, H.-D. (1991) *Biochim. Biophys. Acta 1068*, 195−200.
24. Keller, S. L., Gruner, S. M., and Gawrisch, K. (1996) *Biochim. Biophys. Acta 1278*, 241−246.
25. Blondelle, S. E., and Houghten, R. A. (1991) *Biochemistry 30*, 4671−4678.
26. Oren, Z., and Shai, Y. (1997) *Biochemistry 36*, 1826−1835.
27. Ladokhin, A. S., and White, S. H. (1999) *J. Mol. Biol. 285*, 1363−1369.
28. Perez-Paya, E., Houghten, R. A., and Blondelle, S. E. (1994) *Biochem. J. 299*, 587−591.
29. Sharon, M., Oren, Z., Shai, Y., and Anglister, J. (1999) *Biochemistry 38*, 15305−15316.
30. Oblatt-Montal, M., Buhler, L. K., Iwamoto, T., Tomich, J. M., and Montal, M. (1993) *J. Biol. Chem. 268*, 14601−14607.
31. Bechinger, B., Zasloff, M., and Opella, S. J. (1993) *Protein Sci. 2*, 2077−2084.
32. Dufourcq, J., and Faucon, J.-F. (1977) *Biochim. Biophys. Acta 467*, 1−11.
33. Batenburg, A. M., Hibbeln, J. C. L., and de Kruijff, B. (1987) *Biochim. Biophys. Acta 903*, 155−165.
34. Jacobs, R. E., and White, S. H. (1989) *Biochemistry 28*, 3421−3437.
35. Marsh, D. (1981) in *Membrane Spectroscopy* (Grell, E., Ed.) Springer-Verlag, Berlin.
36. Marsh, D. (1985) *Prog. Protein−Lipid Interact. 1*, 143−172.
37. Kleinschmidt, J. H., Mahaney, J. E., Thomas, D. D., and Marsh, D. (1997) *Biophys. J. 72*, 767−778.

BI000570B